China's carbon budget inventory from 1997 to 2017 and its challenges to achieving carbon neutral strategies

Sirui Zhang [a,b], Xiaoyong Bai [a,b,d,*], Cuiwei Zhao [b], Qiu Tan [b], Guangjie Luo [e], Luhua Wu [a,c], Huipeng Xi [a,c], Chaojun Li [a], Fei Chen [a,f], Chen Ran [a,b], Min Liu [a,b], Suhua Gong [a], Fengjiao Song [a]

[a] State Key Laboratory of Environmental Geochemistry, Institute of Geochemistry, Chinese Academy of Sciences, Guiyang, 550081, China
[b] School of Geography and Environmental Sciences, Guizhou Normal University, Guiyang, 550001, Guizhou Province, China
[c] Puding Karst Ecosystem Observation and Research Station, Chinese Academy of Sciences, Puding, 562100, China
[d] CAS Center for Excellence in Quaternary Science and Global Change, Xi'an, 710061, Shanx Province, China
[e] Guizhou Provincial Key Laboratory of Geographic State Monitoring of Watershed, Guizhou Education University, Guiyang, 550018, China
[f] College of Resources and Environmental Engineering, Guizhou University, Guiyang, 550025, China

ARTICLE INFO

ABSTRACT

The global climate change situation partly depends on the climate change policies of countries around the world, including China. Therefore, it is necessary to reasonably reduce carbon emissions (CEs) and increase carbon sink in order to progressively achieve the carbon neutral (CN) goal. However, the capacity and the potential to achieve carbon neutral with the support of its ecosystem, that is to say the carbon neutral capacity (CNC) and potential, are still unclear. To this end, based on China's energy emissions data, meteorological and hydrological data, lithology data, and vegetation data, we used the GEM-CO_2 model, soil respiration model, spatial auto-correlation analysis method and other methods to establish the spatial information map of China city-scale CNC from 1997 to 2017. Furthermore, based on the future climate, vegetation data, CEs data and their influencing factors in 2025–2060, the Back Propagation neural network model was used to predict the CN potential of China's provinces. This study found during the study period, annual CEs of 5.63 Pg CO_2 were not absorbed, which is about 90% of the average annual CEs. And the carbon surplus regions were mainly concentrated in the less developed northeastern and southwestern border regions. Moreover, the change in the CNC in China from 1997 to 2017 was −13.37 Tg/yr, indicating that the CNC of China's terrestrial ecosystems overall reduced. It should be noted that most provinces are not highly polarized, that is, there is no significant differences in CNC between cities in the provinces. Moreover, the scenario simulation's method of IPCC provides a reference for this manuscript, so we set up two future scenarios (A2 and B1 scenarios). In the future, China is expected to achieve a carbon emission peak before 2030 under the B1 scenario while it will continue to grow under the A2 scenario. From 2017 to 2060, the CNC under the two scenarios (A2/B1) will decrease by 44.58% and increase by 15.54%. It follows then that the road to CN in China will be difficult without corresponding policy intervention. In short, this study has clarified China's CNC from the past to the future, as well as CNC's spatial distribution and changing trends. This provided theoretical and data support for China to introduce corresponding zero-carbon solutions based on its understanding of CNC.

1. Introduction

In September 2020, China announced its goal of addressing climate change, which is to achieve a peak in carbon emissions (CEs) based on energy consumption by 2030 and carbon neutral (CN) by 2060. However, China's CEs have exceeded 10 Pg and not yet reached the carbon peak stage. Moreover, the speed of achieving net zero in 40 years has not

been tried by other countries (Mallapaty, 2020). Therefore, the road to CN in China will be arduous and rapid in the foreseeable future. In order to achieve this goal, at the same time as deep emission reduction, China focus on nature-based solutions to form a green and low-carbon model: reducing energy consumption and increasing ecosystem carbon sink (ECS). So China urgently needs to formulate corresponding policies regarding zero-carbon projects based on understanding the carbon

neutral capacity (CNC). When CNC (ECS-CEs) is a positive value, it means that the place is in a state of carbon surplus and has achieved CN. On the contrary, when CNC is a negative value, it is in a state of carbon deficit and lacks the capacity to offset CEs. Previous studies have shown that the largest total carbon exchange in the world occurs at the interface between the atmosphere and the terrestrial biosphere (Solomon et al., 2007). Nearly 43% of the CO_2 emitted by human activities remains in the atmosphere, 22% is removed by the ocean, and 29% is removed by terrestrial ecosystems (Friedlingstein et al., 2019). In addition, many scholars have also found that continental rock weathering carbon sink (RCS) account for 30% of the missing carbon sink (Ciais et al., 2013; Xi et al., 2021). Thus, in addition to improving technology for reducing CEs, carbon sequestration in ecosystems can offset the global climate problems caused by human development.

The International Biology Program (IBP) in 1964 was the beginning of the global study of carbon storage in terrestrial forest ecosystems (Worthington, 1965). Carrie et al. (1996) affirmed the role of forests in absorbing CO_2. In addition, he has also repeatedly proposed that forests can be used to achieve the storage of CO_2, but due to a lack of biomass calculations, it is impossible to quantify the role of vegetation carbon sink (VCS; Lapenis and Klene, 1997). In order to accurately quantify VCS, Foley (1995) and Fang (2000) proposed using forest area and biomass per unit area to calculate the magnitude of the sink. Then, Goulden et al. (1998) determined that a deciduous broad-leaved forest in New England, USA, has a large carbon sink capacity of 1.4–2.8 t $C \cdot hm^{-2}/yr$ based on the Eddy variance method. The net ecosystem productivity (NEP) is also an important indicator for measuring the size of the ECS. Therefore, Zhang et al. (2020) used the method of estimating the NEP and found that the ECS in China was 0.134 Pg C/yr.

RCS is also an important part of global terrestrial ecosystems (Ciais et al., 2013). The ions formed by the weathering of rocks eventually become sedimentary carbonate minerals and flow into the ocean, thereby removing CO_2 from the atmosphere (Tao et al., 2011). Based on the Intergovernmental Panel on Climate Change's (IPCC) fifth climate change assessment report, RCS is listed as one of the 4 methods of CO_2 removal (Pu et al., 2015). Using the greenhouse gas emissions (GEM)-CO_2 model, Gong et al. (2020) found that the RCS in China was about 20% of the ECS. In addition, based on the same method, Xi et al. (2021) showed that the global RCS was 0.32 ± 0.02 Pg C. Therefore, the RCS is of great significance to the carbon cycle and carbon budget (Liu, 2000; Martin, 2017; Li et al., 2018).

As CEs is a key factor leading to climate change, it has attracted the attention of many researchers (Lin and Benjamin, 2017). The consumption of different energy sources multiplied by the emissions factor is a method of calculating the CEs, generally on the international scale. In terms of CE prediction, the impact, population, affluence, technology (IPAT) model, market allocation-macroeconomic (MARKAL-MACRO) model, long range energy alternatives planning (LEAP) model, and stochastic impacts by regression on population, affluence, and technology (STIRPAT) model have been widely used to predict China's CEs (Xi et al., 2014; Zhou and Mi, 2010; Yang, 2017). For example, Qu and Guo (2010) used the STIRPAT model to predict that China's CEs will reach a peak in 2020–2045. Song and Zhang (2011) applied the neural network method to show that during the Twelfth Five-Year Plan period, the growth rate of the gross domestic product (GDP) should be appropriately reduced to accelerate the fulfillment of the emissions targets.

For achieving the goal of CN, we desperately need to assess the status quo of China's CNC so that the government can use it as a basis to formulate corresponding policies and systems. Furthermore, to accurately estimate China's CNC, it is necessary to precisely evaluate China's ECS and anthropogenic CEs. However, the current accurate estimation of the overall carbon sinks of China's terrestrial ecosystems is incomplete, and the distribution of the ECS is not clear. First, the previous analyses of the temporal and spatial patterns of the ECS considered forest and soil but ignored rocks, which are a huge missing carbon sink, especially in karst areas where carbonate rocks are widely distributed.

Second, most scholars have only focused on carbon sources or carbon sinks, thus ignoring the investigation and quantification of the overall situation of China's carbon budget. Finally, there is also a lack of relevant research on the evaluation of the future performance of China's CNC under different scenarios.

The main goals of this study are to resolve the incompleteness of China's carbon budget, investigate the temporal and spatial distribution process, and resolve the lack of future scenario simulations and predictions. Based on China's energy emissions data, meteorological and hydrological data, lithology data, and vegetation data, we used the GEM-CO_2 model, soil respiration model, spatial autocorrelation analysis method, neural network model, and other methods to reveal the temporal and spatial distributions of the ECS in China, to explore the differences in the CNC in different regions of China, and to simulate and predict the CN potential under future scenarios. This is essential to gaining a better understanding of the carbon cycle, supporting the formulation of climate policies, and predicting future climate change.

2. Material and method

2.1. Data source

2.1.1. Carbon emissions and driving factor data

The data from CEs accounts and datasets (CEADs) used particle swarm optimization-back propagation (PSO-BP) algorithm to unify DMSP/OLS and NPP/VIIRS satellite imagery, and estimate the CO_2 emissions of 2735 counties in China from 1997 to 2017. During this period, China city-level CEs data set was organized by this study (Chen et al., 2020).

According to the widely used logarithmic mean divisia index (LMDI) model, the CE driving factors were determined (He, 2019). The population and urbanization rate were selected as the population scale indicators; GDP and the proportion of the secondary industry were used as the economic level indicators; energy intensity, total energy use and energy structure were regarded as the technical level indicators. The above data were obtained from the statistical yearbook of the National Bureau of Statistics of China (NBSC, 2021). According to the research of He (2019), this study set the growth rate in the CEs of impact factors from 2025 to 2060 (Tables S1–4).

2.1.2. Climate data

The resolution of temperature and precipitation data from 1997 to 2017 is 1 km (Peng et al., 2019). This set of data was based on the Chinese mean temperature (2 m) and precipitation data set (1 km) published by Climatic Research Unit (CRU) and the climate data set published by WorldCLIM. In addition, the data of 496 independent meteorological observation points were used for verification, and the verification results were credible. The 1 km evapotranspiration data is the Chinese surface evapotranspiration product (v1.5) established by the evapotranspiration complementary method (http://www.geodata.cn). The temperature and precipitation data from 2025 to 2060 come from the future monthly climate data of the National Center for Atmospheric Research (https://ncar.ucar.edu/), including two scenarios (A2 and B1) with a resolution of 0.5°. In addition, the evapotranspiration data for this time period is driven by the future climate change data released by CRU and simulated by using the Integrated Biosphere Simulator (IBIS) model. The data has been extensively verified by comparison (Zhen et al., 2013).

2.1.3. Vegetation and lithology data

The net primary production (NPP) data in China comes from the monthly composite products of the MOD17A3 datasets from the Land Processes Distributed Active Archive Center (Running et al., 2015), with a spatial resolution of 1 km and a time span of 2000–2017. Due to the lack of MODIS data before 2000, China's NPP data from 1997 to 1999 was based on the Carnegie-Ames-Stanford approach (CASA) model, with

input including solar radiation, normalized vegetation index, temperature and water stress factors and other parameters (Chen et al., 2019). The NPP data from 2025 to 2060 was driven by the global historical period weather data released by the CRU Meteorological Center, and was obtained by using the IBIS model to simulate in different scenarios of A2 and B1 (http://www.geodata.cn). In addition, the data has been extensively verified by comparison (Zhen et al., 2013).

The lithology distribution map and various lithology coefficients in China come from the global lithology database with a spatial resolution of 0.5° (Hartmann and Moosdorf, 2012).

2.2. Method

2.2.1. Carbon emissions model

In the "2006 IPCC Guidelines for National Greenhouse Gas Inventories" (IPCC, 2006), the IPCC detailed three methods for estimating CEs from fossil fuel combustion in stationary and mobile sources. This study selected the first method to calculate national CEs. The specific method is as follows:

$$CO_2 = \sum_{i=1}^{14} CO_{2,i} = \sum_{i=1}^{14} E_i \times NCV_i \tag{1}$$

CO_2 represents CEs to be estimated; i represents various energy fuels, including coal, coke, coke oven gas, blast furnace gas, converter gas, other gas, crude oil, gasoline, kerosene, diesel, fuel oil, liquefied petroleum gas, Natural gas and liquefied natural gas; E_i represents the combustion consumption of various energy sources; NCV_i is the average low calorific value of various energy sources, used to convert various energy consumption into energy units (TJ); CEF_i represents the CEs of various energy sources factor.

2.2.2. Calculation method for NEP

Net ecosystem productivity (NEP) was first proposed by Woodwell et al. (1978), which referred to NPP minus the photosynthetic product consumed by heterotrophic organisms (soil respiration). NEP represents the net storage of carbon on a larger scale. When NEP is greater than 0, it means that the ecosystem is a sink of CO_2, otherwise it is a source. The formula is as follows:

$$NEP = NPP - RH \tag{2}$$

where, NPP means net primary productivity (kg m^{-2} yr^{-1}), and RH means heterotrophic respiration (kg m^{-2} yr^{-1}). In order to invert RH to a larger spatial scale, the regression equation of temperature, precipitation and CEs was used to calculate it (Pei et al., 2009):

$$RH = 0.22 \times (e(0.0913 \times T) + \ln(0.3145 \times R + 1)) \times 30 \times 46.5\% \tag{3}$$

T is the average surface temperature (°C) and R is the precipitation (mm).

2.2.3. GEM_CO$_2$ method

The "Global Erosion Model of CO_2 Flux" (GEM-CO_2) model is a method for estimating the latitudinal distribution of carbon consumed by global chemical weathering using lithology and continental basin maps (Suchet et al., 2003). The model takes runoff as the main influencing factor of global chemical weathering, and obtains the relationship between different lithological weathering rates and runoff, thereby establishing a simple model based on empirical coefficients.

$$F_{co_2} = aQ \tag{4}$$

where Q represents the runoff (mm) and a is the empirical coefficients of silicate rock types.

2.2.4. Back Propagation (BP) neural network model

The Back Propagation (BP) neural network model proposed by Rumelhart and Mcclelland (1987) is currently a more widely used multilayer feedforward neural network model. It can fit nonlinear functions with arbitrary precision. The topology of the BP neural network model includes an input layer, a hidden layer, and an output layer. The population, urbanization rate, GDP, the proportion of the secondary industry, energy intensity, total energy use and energy structure were selected as seven input layers. The output layer was CEs. After many adjustments, 4 hidden nodes were set to obtain network structures of [5 4 8 6]. Finally, CEs data with good fitting effect was outputted from the model.

In the model, the output formula of the hidden layer neuron is:

$$Out_j = f\left(\sum_{i=1}^{m} W_{ji}^1 X_i - \theta_j^1\right), \quad j = 1, 2, 3........ \tag{5}$$

Out represents the hidden layer neuron, f(x) is the transfer function (ReLU function) of the hidden layer, and W^1 represents the network weight matrix between the input layer and the hidden layer.

The output formula of the output layer neuron is:

$$Z_k = g\left(\sum_{i=1}^{m} W_{kj}^2 O_j - \theta_k^2\right), k = 1, 2, 3....... \tag{6}$$

Z represents the output layer neuron, g(x) is the transfer function (linear function) of the output layer, and W^2 represents the network weight matrix between the hidden layer and the output layer.

In order to finally test the reliability of the fitting results, this study chose the coefficient of determination (R^2) as the corresponding index. Then, the closer R^2 is to 1, the better the performance of the prediction model.

2.2.5. Hurst index

The Hurst index can quantitatively describe the degree of dependence of sequence length and describe the degree of sustainability through numerical grading. In this study, the aggregate variance method was used to calculate the Hurst index of CNC changes. The formula is as follows:

$$X_m(k) = \frac{1}{m} \sum_{i=(k-1)m+1}^{k_m} x_i, k = 1, 2..., [N/m] \tag{7}$$

Then the sample variance of their mean is calculate:

$$V_{ar}X_m = \frac{1}{N/m} \sum_{k=1}^{N/m} [X_m(k) - \overline{X}]^2 \tag{8}$$

The slope interval can be divided into the following three situations (Walter, 1994): (1) If $0 \leq H \leq 0.5$, it indicates that the change of CNC time series has reverse persistence, and the more H value tends to 0, the stronger anti-persistence. (2) If H = 0.5, the correlation degree before and after the correlation time series is weak; (3) If $0.5 \leq H \leq 1$, it indicates that the time series change has positive persistence, and the value of H tends to 1, the stronger the persistence.

2.2.6. Trend analysis method

This paper uses the pixel-by-pixel unitary regression trend analysis method to analyze the evolution trend of various indicators of China's carbon budget during the research period. If the slope is greater than 0, it indicates that these indicators are upward trend during the study period, and vice versa. And the larger the magnitude of absolute value of the slope is, the faster the change is. The formula is as follows:

$$\theta = \frac{n \times \sum_{i=1}^{n}(i \times X_i) - \left(\sum_{i=1}^{n} i\right)\left(\sum_{i=1}^{n} X_i\right)}{n \times \sum_{i=1}^{n} i^2 - \left(\sum_{i=1}^{n} i\right)^2} \tag{9}$$

Where θ is the evolution trend, i is the serial number of the year, n is the research period, and Xi is the indicator in the i-th year.

2.2.7. Mann—Kendall method

Mann–Kendall (M–K) trend analysis is a method to detect the changing trend of a series (Kendall, 1975; Mann, 1945), without the need for a specific distribution test on the data series. In the method, UFk stands for sequential time series and UBkc stands for sequential time series. If the value of UFk or UBk is greater than 0, it indicates that the sequence has an upward trend, and if it is less than 0, it indicates a downward trend. When they exceed the critical straight line, it indicates a significant upward or downward trend. The range beyond the critical line is determined as the time zone where the sudden change occurs. If the two curves of UFk and UBk have an intersection point, and the intersection point is between the critical lines, then the time corresponding to the intersection point is the time when the sudden change begins.

2.2.8. The spatial autocorrelation analysis

By using spatial autocorrelation analysis, the spatial dependence and agglomeration patterns of CNC in China were obtained. Spatial autocorrelation (including global and local spatial autocorrelation) can indicate the degree of interdependence and aggregation between attributes in a specific area and attributes in other areas. The Moran's I index is used to analyze the overall spatial agglomeration of the entire study area (Moran, 1950), as shown in the equation (10). The local index of spatial correlation (Anselin, 1995) reflects a large extent the spatial correlation between the spatial attribute and its neighboring spatial attribute value, as shown in the equation (11).

$$Moran'sI = \frac{\sum_{i=1}^{n}\sum_{j=1}^{n}Wij(xi-\overline{x})(xj-\overline{x})}{S^2\sum_{i=1}^{n}\sum_{j=1}^{n}Wij} \quad (10)$$

$$LocalMoran'sI = \frac{n(xi-\overline{x})\sum_{j=1}^{m}Wij(xj-\overline{x})}{\sum_{i=1}^{n}(xi-\overline{x})^2} \quad (11)$$

where n represents the number of cities in China, m is the number of cities adjacent to city$_j$ in space, $i \neq j$; $S = \frac{1}{n}\sum_{i=1}^{n}(xi-\overline{x})^2$; xi and xj represent the CNC of cities i and j; Wij represents the spatial weight matrix of i and j; $\overline{x}$ is the average CNC. The value of I is between −1 and 1, and the higher the absolute value of I, the stronger the spatial autocorrelation reflected. When I > 0, there is a positive spatial correlation; when I < 0, there is a negative spatial correlation; when I = 0, there is no spatial autocorrelation. Local autocorrelation includes four types: high-high (HH), low-low (LL), high-low (HL) and low-high (LH), which respectively represents the collection of units with high CNC, the collection of units with low CNC and units with high (or low) CNC are surrounded by units with low (or high) CNC.

2.2.9. The Gini coefficient

At present, the Gini coefficient is widely used in the field of CEs research to measure its distribution characteristics (Chen et al., 2016; Clarke-Sather et al., 2011; Liu et al., 2019). Therefore, this study used the Gini coefficient to analyze the degree of polarization of China's CNC. Based on the distribution function, the calculation formula is:

$$G = \int_{min}^{max} F(x)(1-F(x))dx \Big/ \mu \quad (12)$$

where the probability density function of the CNC (X) is $f(x)$, min < x < max. In this formula, min and max indicate the lower limit (can be negative) and upper limit of the X. In addition, the distribution function of the X is $F(x) = \int_{min}^{x} f(t)dt$ and expectation is $\mu = \int_{max}^{min} xf(x)dx$.

Since the CNC has a negative value, it is divided into three cases: carbon deficit, carbon surplus, and CN to calculate the Gini coefficient (Ai, 2017). The CNC function should be segmented function:

$$F(x) = \begin{cases} P_1F_1, & min < x < 0 \\ 1 - P_2, & x = 0 \\ 1 - P_2 + P_2F_2, & 0 < x < max \end{cases} \quad (13)$$

where P_1, $1 - P_1 - P_2$ and P_2 are the proportions of the three municipal administrative regions in the province, with carbon deficit, carbon surplus, and CN. The sum of the three equals 1. $F_1(x)$ and $F_2(x)$ are the distribution function of CNC of the case of carbon deficit and carbon surplus respectively in each cities.

According to formula (1), their distribution function can be derived. The calculation formula is as follows:

$$G1 = \int_{min}^{0} F_1(x)(1-F_1(x))dx \Big/ |\mu_1| \quad (14)$$

$$G2 = \int_{0}^{max} F_2(x)(1-F_1(x))dx \Big/ |\mu_2| \quad (15)$$

in the above formulas, G1 is the Gini coefficient for the carbon deficit, G2 is the Gini coefficient for the carbon surplus, and the Gini coefficient for CN is 0. Therefore, the overall Gini coefficient is:

$$G = \int_{min}^{0} F_1(x)(1-F_1(x))dx \Big/ |\mu_1| + \int_{0}^{max} F_2(x)(1-F_1(x))dx \Big/ |\mu_2| \quad (16)$$

3. Results

3.1. Spatial pattern and changes in the terrestrial ecosystem carbon sink in China

The NEP and RCS are the main carbon sequestration pathways in terrestrial ecosystems, so the ECS is the sum of the NEP and the RCS. This study drew a more comprehensive map of the ECS distribution in China (Fig. 1), as well as the different continental carbon sink processes.

This study showed that China's terrestrial ecosystem was a huge carbon sink from 1997 to 2017, and its annual average NEP reached 0.61 Pg CO_2/yr. In 2000, the NEP rose sharply (Fig. 1d). This was due to the large-scale ecological restoration project implemented in the 21st century in China (Lythgoe et al., 2007; Pan et al., 2011). In terms of distribution, the two sides had opposite effects on the NEP with the Hu Huanyong line as the boundary. To the southeastern of the boundary, the carbon sink was greater than the respiration, exhibiting a carbon sink state overall, while the area to the northwest of the boundary became a huge carbon source (Fig. 1a). In the carbon sink regions, the higher NEP regions were mainly distributed in Yunnan, Sichuan, and Heilongjiang, and they were 152.78 Tg, 73.41 Tg, and 61.30 Tg respectively. Among them, Yunnan is rich in natural resources and contains a wide area of vegetation, so the NEP was particularly prominent. In addition, the provinces that were carbon source regions were Tibet, Xinjiang, Qinghai, Ningxia, and Tianjin. Among them, the NEP in Tibet was more than 100 times that in Tianjin.

In addition to the vegetation and soil carbon sink in the ecosystem, the IPCC pointed out that rock weathering is also a main carbon sink (Pu et al., 2015). The RCS in China was 10 Tg C/yr. As can be seen from Fig. 1b, the RCS varied significantly spatially. The RCS high values were mainly distributed in southwestern China. For example, due to the warm climate, abundant precipitation, and widespread carbonate rocks, the RSC has further increased Guangxi's CO_2 absorption (6.14 Tg), accounting for 10% of the RCS in China.

From 1997 to 2017, the ECS exhibited a slow upward trend, with an
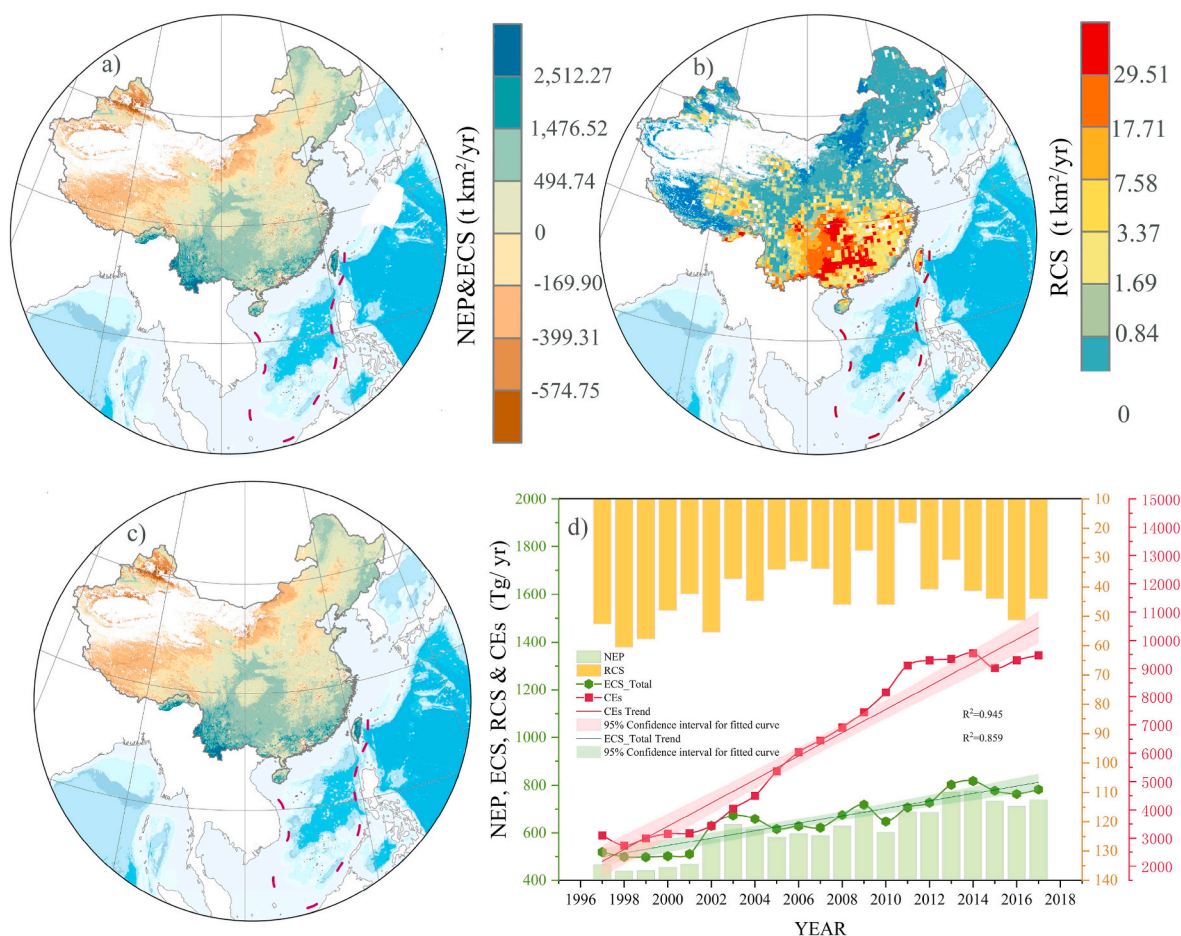
Fig. 1. The spatial pattern of the terrestrial ecosystem carbon sink (ECS) in China (b), including the net ecosystem productivity (NEP) (a) and rock weathering carbon sink (RCS) (b). The time evolution of them and carbon emissions (CEs) (d). (In the Fig. 1d, these data exclude Tibet, Hong Kong, Macau and Taiwan; green axis is NEP and ESC, organ axis is RCS and red axis is CEs).

average annual growth rate of 2.77%. The minimum occurred in 1998 (0.12 Pg C/yr), and the maximum occurred in 2014 (0.21 Pg C/yr). The RCS was stable, with slight fluctuations, during this period. China's CEs rose sharply year by year from 1997 to 2017, with an average annual rate of change of 9.81%, which was about four times the change in the ECS. In addition, the ECS is a natural background resource, so it only can alleviate the pressure of CN to a certain extent. Since 2005, the gap between the CEs and ECS has continued to widen.

3.2. Spatial pattern of the carbon neutral capacity in China

During the study period, annual CEs of 5.63 Pg CO_2 were not absorbed, which is about 90% of the annual average CEs. However, the entire country was not in a state of carbon deficit. Due to economic factors, the carbon surplus regions were mainly concentrated in the less developed northeastern and southwestern border regions (Fig. 2).

Twenty-eight cities (county-level cities) across the country contributed 117 Tg of ECS in addition to achieving CN. China derived 53.56% of carbon surplus (25.26 Tg) from Yunnan, which contains 11 cities. The top provinces were Heilongjiang, Guangxi, and Gansu, with 12.53 Tg, 7.35 Tg, and 5.51 Tg, respectively. Heilongjiang was the only province located in the north. It should be noted that the top three carbon surplus provinces contributed about 88.5% of the country's carbon surplus. Yunnan was the province with the most cities achieving CN in China.

From 1997 to 2017, the carbon deficit regions were widely distributed within all of the provinces and 325 cities (Fig. 2b). The province with the highest carbon deficit (0.52 Pg/yr) was Shandong Province in northern China, and each of the cities in the province was in a state of carbon deficit.

Based on geographical and economic characteristics, China can be divided into eight economic regions (Development Research Center of the State Council, 2005). The carbon deficit was more serious in the plains and economically developed sections of the coastal areas. The ECS of the northern and eastern coastal areas were much smaller than the CEs, so the carbon deficit in the coastal areas was 0.07–0.52 Pg (Fig. 3). The carbon deficit fluxes of Shanghai and Tianjin were as high as 8.78 t/km²/yr and 27.16 t/km²/yr, respectively (Table S5). The northwestern and southwestern regions showed the opposite pattern. These two regions were the largest carbon sources and carbon sinks in China. Therefore, in the northwest, the terrestrial ecosystems in all of the provinces, except Gansu emitted CO_2, of which Xinjiang was the most significant. In southwestern region the only province (Yunnan) achieved an average annual CN target (24.67 Tg/yr). The CNC fluxes of all of the other provinces, except Chongqing, were greater than −0.8 t/km²/yr (Table S5), which has great potential for achieving CN. Due to the water loss and soil erosion, flooding, and relatively developed economies in the Yellow River Basin and the middle reaches of the Yangtze River, the provinces in these regions experienced carbon deficits, and the carbon deficit in the middle reaches of the Yellow River was more serious (1.11 Pg/yr).

3.3. Temporal evolution of the carbon neutral capacity in China

As shown in Fig. 4, the change in the CNC in China from 1997 to 2017 was −13.37 Tg/yr, indicating that the CNC of China's terrestrial ecosystems generally weakened (Fig. 4a). The year with the weakest
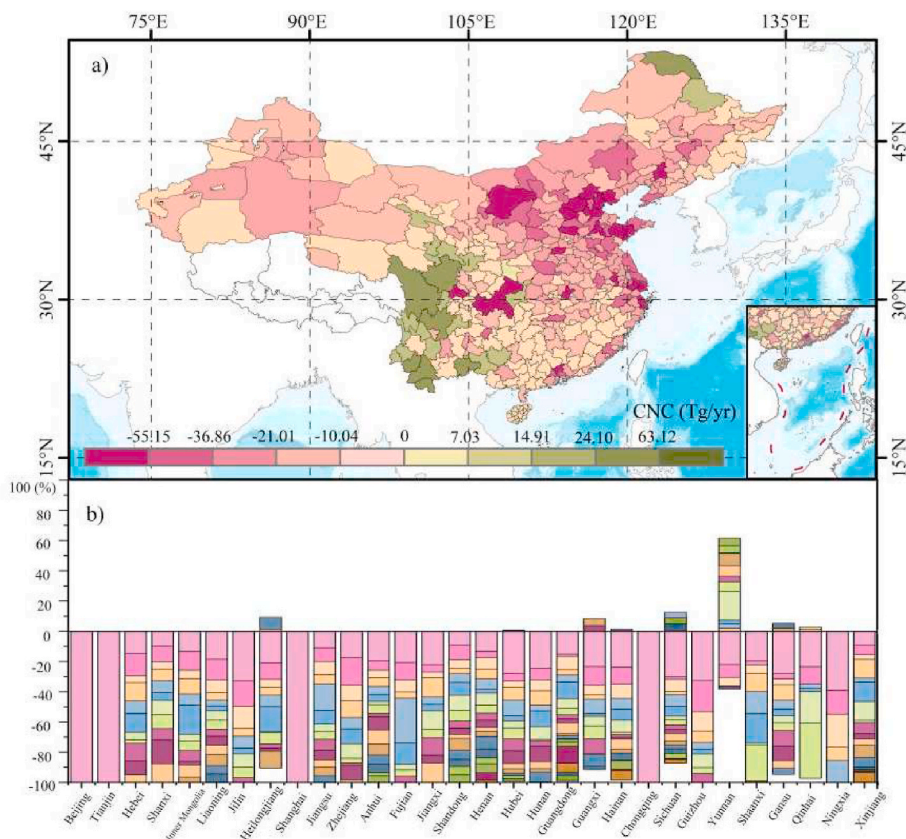
Fig. 2. The spatial distribution (a) of the carbon neutral capacity (CNC) of cities in China and the proportions (b) of the carbon surplus and deficits of the cities (the above data exclude Tibet, Hong Kong, Macau and Taiwan).
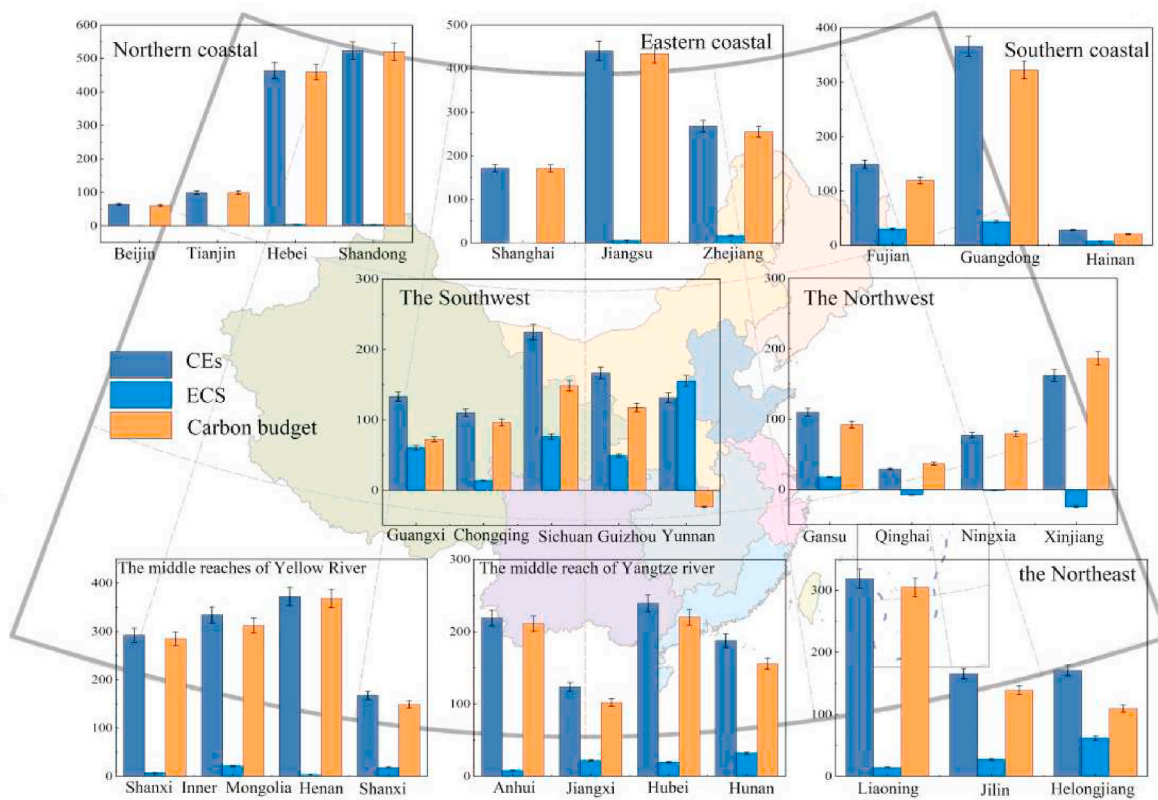

Fig. 3. The current status of the carbon budget in eight economic regions of China (Unit: Tg/yr; a positive value of carbon budget means carbon deficits; the above data exclude Tibet, Hong Kong, Macau and Taiwan).
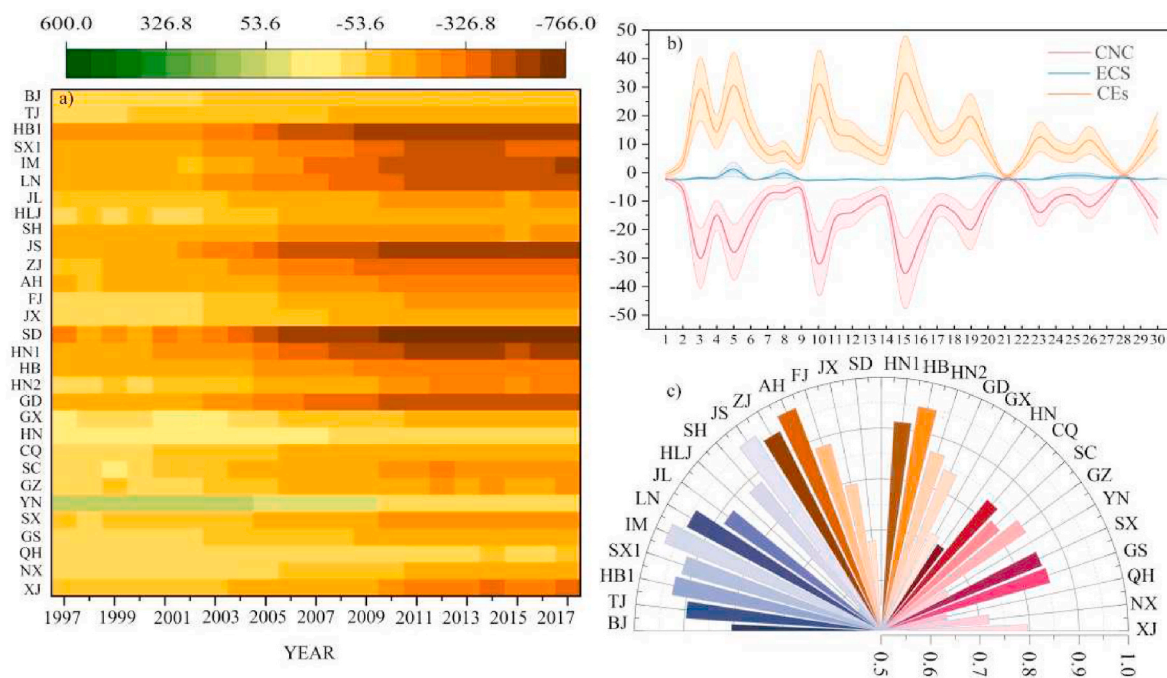
Fig. 4. Time change (a), trend (b), and trend persistence (c) of carbon neutral capacity (CNC) of Chinese provinces from 1997 to 2017 (Unit: Tg/yr; the above data exclude Tibet, Hong Kong, Macau and Taiwan; The sequence of Fig. 4b is the same as that of Fig. 4c).

CNC was 2014 (−8.71 Pg/yr), which was caused by the dramatic increase in the CEs of the country at that time (Fig. 1d). In 1998, China's CNC reached its peak (−2.22 Pg/yr), which was far smaller than China's CN since the beginning of the 21st century. Moreover, the changes in the CNC of various provinces were also quite different due to differences in their natural conditions and the growth rate of their CEs. During the study period, most of the provinces (cities) remained stable as carbon-deficient provinces (Fig. 4a). These provinces, especially Xinjiang and Ningxia, cannot achieve indirect emission reductions in the terrestrial ecosystem, so they can only seek man-made scientific and technological means of achieving the CN targets.

In order to further analyze the changes in China's CNC, ECS, and CEs from 1997 to 2017 and to avoid the randomness and contingency of the analysis results (Lv et al., 2014), the trend analysis method was used to explore these calculation results. In this study, the downward trend was divided into three grades: slight decrease (0 to −10), significant decrease (−10 to −20), and sharp decrease (>−20). Although the CNC of the four municipalities were relatively weak, they also maintained a slight upward trend during the study period (Fig. 4b). This showed that the leading edge of China's economic development was doing its best to achieve the emissions reduction targets. In addition, the trend of maintaining a slight decrease in the CNC exhibited temporal continuity (H > 0.8). As can be seen from Fig. 4, the temporal change in the ECS was maintained at 3.50 Tg/yr to −0.13 Tg/yr, which was much lower than the growth rate of the anthropogenic CEs. Therefore, the CNC of each province was limited by the CEs. The provinces with significant decreases were Guangdong, Liaoning, Zhejiang, Xinjiang, and Shanxi. Among them, Liaoning, Xinjiang, and Shanxi are China's major energy provinces. This showed that in China, economic development and CN goals exist in a state of contradiction. The top five provinces with the strongest decreases in CNC were Shandong, Jiangsu, Hebei, Inner Mongolia, and Henan, which are mainly northern provinces.

From 2001 to 2003, the proportion of heavy industry in the industrial added value increased year by year, reaching 60.6%, 62.6%, and 64.2% in 2001, 2002, and 2003, respectively (Zheng, 2005). This indicated that 2004 was the time node, and China had officially entered a period of heavy industrialization. Thus, with the advent of the heavy

industrialization period, the CNC of most of the provinces in China exhibited a significant downward trend (Fig. S1). The mutation time for Beijing, Inner Mongolia, Qinghai, and other provinces was earlier. Around 2000, the CNC further dropped sharply. The mutation point of the decline in Hainan's CNC was 6 years later than the average mutation time in China. This was because Hainan's economy predominantly relied on tourism, and its industrial development was relatively lagging. In 2010, Hainan's economic growth rate hit a record high since 1994, and its GDP increased by 200 billion yuan (Li, 2021).

3.4. Potential spatial dependence and degree of polarization of carbon neutral capacity

The average CNC of China's cities from 1997 to 2017 was analyzed using the global Moran's I (Fig. 5a), and the results showed that the CNC had a significant positive spatial correlation (Moran's I = 0.315, p = 0). There was an obvious spatial agglomeration characteristic. We further analyzed the local Moran's I and divided the spatial dependence into four types: (1) high values and high value clusters; (2) high values and low value outliers; (3) low values and high value outliers; and (4) low values and low value clusters. The cities in China were dominated by high values and high value clusters and by low values and low value clusters. The spatial boundaries of the distribution of the two were located in the southwestern and the northeastern parts of China, respectively. Both had 99% confidence levels (Fig. 5b). Lanzhou in Gansu Province was the only city in northwestern China whose low CNC was surrounded by high values. In Sichuan, Yunnan, Guizhou, and Guangxi, there were mainly high values and high value clusters. Only in Jiangsu were there low values and low value clusters in the entire territory.

The Gini coefficient is a common index used to measure the degree of polarization of internal indicators in a region. The closer the Gini coefficient to 0, the more equal the CNC of the province. Values of <0.2 are regarded as the absolute average CNC; 0.2–0.3 is regarded as a relatively average CNC; 0.3–0.4 is regarded as a relatively reasonable CNC distribution in the province; and 0.4–0.5 is regarded as a CNC with a large gap. When the Gini coefficient reaches >0.5, there is a great disparity in
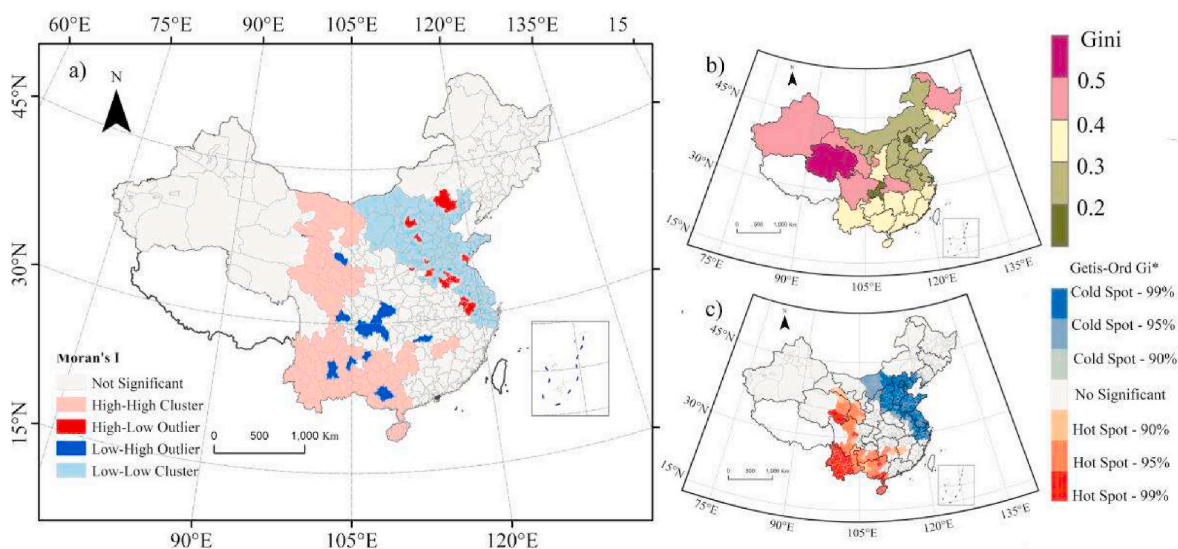
Fig. 5. Potential dependence analysis (a), degree of polarization (b), and the hot and cold spots (c) of carbon neutral capacity (CNC) in China's provinces from 1997 to 2017 (the above data exclude Tibet, Hong Kong, Macau and Taiwan).

the CNC. Most provinces are not highly polarized, that is, there is no significant differences in CNC between cities in the provinces. It should be noted that the CN capacities of the cities in the provinces with weaker CN capacities were also weaker, that is, the area with cold spots corresponded to a low Gini coefficient (Fig. 5b and c). However, Qinghai, Hubei, Sichuan, Gansu, Heilongjiang, and Xinjiang had very large gaps between different cities, with Gini coefficients of 0.53, 0.47, 0.46, 0.45, 0.44, and 0.40, respectively. These provinces all represent regions with large economic differences within provinces. The high growth rates of the economy and industrialization capabilities were mainly concentrated in the provincial capitals and in a few developed prefecture-level cities. This further widened the gap between their CNC. For example, Chengdu is the economic center of Sichuan, with a carbon deficit of 59 Tg, which emitted nearly 30% of the province's CO_2, while the Ganzi Tibetan Autonomous Prefecture in Sichuan had a carbon surplus of 8 Tg and only emitted 4 Tg of CO_2.

4. Discussion

4.1. Comparison with related studies

In recent years, several scholars have separately estimated and analyzed the CEs and ECS. To this end, the IPCC has also established an internationally accepted CEs calculation model. The CEs data used in this study were basically consistent with the data obtained using the IPCC method, with an average relative error of only 5% (Table 1). This demonstrates that the CEs data used in this study were more accurate and reliable.

As can be seen from Table 2, in 2011, Fang et al. (2007) found that the NEP in China was 0.136–0.176 Pg/yr based on the resource inventory, which is slightly smaller than the value obtained in this study. This difference is caused by the author's failure to make a more accurate assessment of the soil carbon sequestration, but the two results still remain at one of the same orders of magnitude, and the difference is not large. In addition, Pan et al. (2011) also found that the carbon sink in China was 0.182 ± 0.45 Pg/yr based on the forest data inventory and the ecological carbon sink mode. The result of this study (0.153 Pg/yr) lies between these estimated values, which demonstrates that our research on the NEP is reasonable. Zhang et al. (2020) used the same research ideas and estimated the value of the NEP from 2001 to 2010 to be 0.134 Pg/yr based on multi-source data, and these results are relatively close. In addition, Piao et al. (2009) used five ecosystem models to

confirm China's huge carbon sequestration potential (0.13–0.22 Pg/yr). The results of this study are between Piao's results for the same time scale. This provides strong scientific support for China to formulate appropriate direct emissions reduction measures based on the goal of CN. Moreover, the results of this study have also been confirmed to be reliable on other regional scales (Pacala et al., 2001) (Table 1).

Qiu et al. (2004) and Gong et al. (2020) used the GEM-CO2 method to estimate the magnitude of the RCS in China, and their results were 14 Tg C and 17.6 Tg C, respectively. These results are slightly larger than the values calculated in this study, but they are both of the same order of magnitude. This situation may be caused by differences in the runoff calculation methods and the spatial resolution. In this study, higher precision (1 km) raster data were used, so our value more clearly reflects the changes in the regional runoff, but the carbon sink value will be slightly smaller. However, Liu and Zhao (2000) and Xu and Jiang (1997) calculated that the RCS in China was 0.48–1.78 Tg C based on the hydrochemical runoff law. The magnitude of the carbon sink obtained in this study is also within the range of their results, and the differences in research period, data sources, and accuracy may also lead to small differences in the results.

In summary, the comparison presented above shows that the results of this study are reliable. This model is reasonable and reliable in terms of the calculation of China's CNC. It can more accurately quantify the temporal and spatial patterns of the CNC in the different regions of China.

4.2. Comparison of carbon neutral capacities of China and other countries

From 2000 to 2015, China made great achievements in reducing emissions. The carbon intensity in China was in a period of rapid decline, from 2.60 kg/USD in 2000 to 0.81 kg/USD in 2015, i.e., an average annual decrease of up to 11% (Fig. 6a). However, there was still a large gap compared with developed countries. In 2015, China's CEs intensity was 2.74 times that of the United States and 2.92 times that of Japan. Therefore, the 14th Five-Year Plan proposes to "implement a system with carbon intensity control as the mainstay and total CEs control as a supplement." It is necessary to start by adjusting the industrial structure, optimizing the energy consumption structure, and accelerating the economic transformation (Ping et al., 2020).

However, in terms of per capita CEs, China's was lower than the United States, Japan, and Russia, and the annual average level was only

Table 1

Comparison of the carbon emissions (CEs) in this paper with the IPCC results.(carbon emission accounts and datasets (CEADs); International Panel on Climate Change (IPCC)).

Location	1997		2010		2017		MEAN	
	IPCC	CEADs	IPCC	CEADs	IPCC	CEADs	IPCC	CEADs
Beijing	61.9	42.5	103.0	90.9	85.0	60.1	86.8	64.0
Tianjin	51.4	52.9	136.6	123.9	141.0	150.0	104.9	99.0
Hebei	212.1	225.6	647.0	594.8	726.0	682.4	502.1	463.6
Shanxi	148.7	156.1	406.5	374.1	488.0	397.6	327.1	292.2
Inner Mongolia	97.0	117.0	477.4	465.7	639.0	573.5	351.9	334.1
Liaoning	200.7	174.6	446.3	405.7	479.0	433.5	341.8	318.8
Jilin	98.6	93.2	202.1	213.8	204.0	227.7	158.9	165.4
Heilongjiang	129.1	86.3	218.3	217.5	269.0	225.4	190.4	170.7
Shanghai	103.2	109.1	187.1	230.7	190.0	192.5	160.6	171.5
Jiangsu	183.9	186.4	580.3	583.8	736.0	669.7	451.8	440.3
Zhejiang	115.4	117.3	358.6	373.5	382.0	369.6	272.3	271.9
Anhui	109.5	105.7	261.9	282.8	371.0	322.9	222.1	218.8
Fujian	44.2	68.2	199.4	188.4	230.0	230.0	147.8	149.2
Jiangxi	51.8	57.8	148.4	150.0	224.0	212.5	124.9	123.6
Shandong	199.3	320.4	766.6	727.6	806.0	766.6	557.2	523.5
Henan	154.3	175.9	504.7	475.9	494.0	551.3	364.0	372.2
Hubei	133.9	130.4	324.3	305.4	325.0	329.0	238.0	239.2
Hunan	98.0	82.9	254.9	231.8	310.0	311.5	194.7	187.5
Guangdong	165.1	171.3	471.5	469.0	542.0	514.6	369.9	366.2
Guangxi	50.8	59.5	171.8	162.5	221.0	231.8	129.5	133.2
Hainan	7.2	13.0	28.9	19.5	42.0	39.6	24.0	20.6
Chongqing	55.4	63.2	141.5	141.0	158.0	153.8	109.3	110.2
Sichuan	123.1	106.9	303.8	291.7	309.0	331.1	221.5	224.7
Guizhou	72.2	87.3	191.5	207.5	255.0	253.6	161.3	166.7
Yunnan	58.0	60.6	194.2	167.9	195.0	211.9	136.3	131.6
Shaanxi	68.9	69.6	218.6	216.3	262.0	275.4	162.5	167.3
Gansu	50.3	54.0	126.5	138.2	151.0	171.4	102.2	109.9
Qinghai	11.5	17.8	31.8	28.3	53.0	58.1	29.6	29.3
Ningxia	17.1	32.0	95.3	81.6	175.0	168.6	82.3	77.5
Xinjiang	63.2	53.0	167.6	190.5	404.0	340.7	168.6	162.2
Total	2935.8	3090.5	8366.4	8150.3	9866.0	9456.4	6494.1	6304.9

Table 2

Comparison of NEP magnitude in China with other research results.

Region	Method	NEP (Pg C/yr)	Study period	Reference
China	Bottom-up process	0.182 ± 0.45	2000–2007	Pan et al. (2011)
	Resource inventory	0.136–0.176	1981–2000	Fang et al. (2007)
	NPP-RH	0.134	2000–2015	Zhang et al. (2020)
	Ecosystem models	0.13–0.22	1980–2002	Piao et al. (2009)
United States	The tracer-transport inversion method	0.30–0.58	1980–1989	Pacala et al. (2001)
China	This study	0.12–0.21	1997–2017	
	This study	0.120–0.127	1997–2000	
	This study	0.153	2000–2007	
	This study	0.172	2000–2015	
United States	This study	0.39	2000–2015	

25% that of the United States. However, during this period, the per capita CEs in the United States exhibited a continuous downward trend through the turning point (Fig. 6b). As a newly industrialized country, China was continuously increasing its per capita CEs due to industrialization, urbanization, and improved living patterns (Diakoulaki et al., 2006; Talukdar and Meisner, 2001). In addition, the rate of decrease of the CNC in China far exceeded those of the above three countries, and its ECS was the lowest, except for Japan, which has small resources (Fig. 6c and d). We should consider that economic development is important, but economic growth alone cannot bring about environmental sustainability (Yang et al., 2021; Cumming and von Cramon-Taubadel, 2018). Therefore, achieving the inflection point of per capita CEs as soon as possible should be a policy goal.

4.3. Future scenario forecast of China's carbon neutral capacity

By exploring the future potential of China's CN, this study hoped to understand emissions in China in order to provide theoretical support for the more effective implementation of greenhouse gas emissions reduction. In this study, population size, economic level, and technological level were considered to be the driving factors of CEs, and the CEs in different years were used as the output parameters. Finally, a back propagation (BP) neural network model was used to predict China's CEs from 2025 to 2060. We have envisaged two scenarios for the future, where A2 is a regional development scenario, and B1 is a global sustainable development scenario (Intergovernmental Panel on Climate Change, 2000). The test results of the neural network model showed that in the verification of the test samples, the relative errors of the CEs in the two scenarios were within 10% (Fig. S2). Among them, 90% of the annual CEs had a relative error of less than 5%. This proved that the model had certain accuracy in predicting China's CEs. So the results indicated that under scenario A2, CEs will continue to increase in the future, and the goal of reaching peak CEs will still not be achieved by 2030 (Fig. 7). Moreover, China's CEs will exceed 13 Pg in 2060. In scenario B1, China's CE rate will increase enormously because some high-tech industries and service industries will emerge, and the demand for infrastructure investment will continue to increase (Wang and Lin, 2017, Wang et al., 2018). As a result, CEs will soar and exceed 20 Pg, but the carbon peak will eventually be achieved in 2029 through the establishment of a mature sustainable development system, which will reduce CEs to 8 Pg in 2060 and return to the 2010 CEs level. Therefore, scenario B1 is more in line with the long-term development goals. In view of this fact, if the industrial structure and other aspects are not adjusted, China's rapid economic growth will occur at the expense of natural resources and the environment (Hatfield-Dodds et al., 2015).

Using the IBIS model to calculate the NPP, in this study, the future ECS was also divided into two scenarios, A2 and B1. As can be seen from
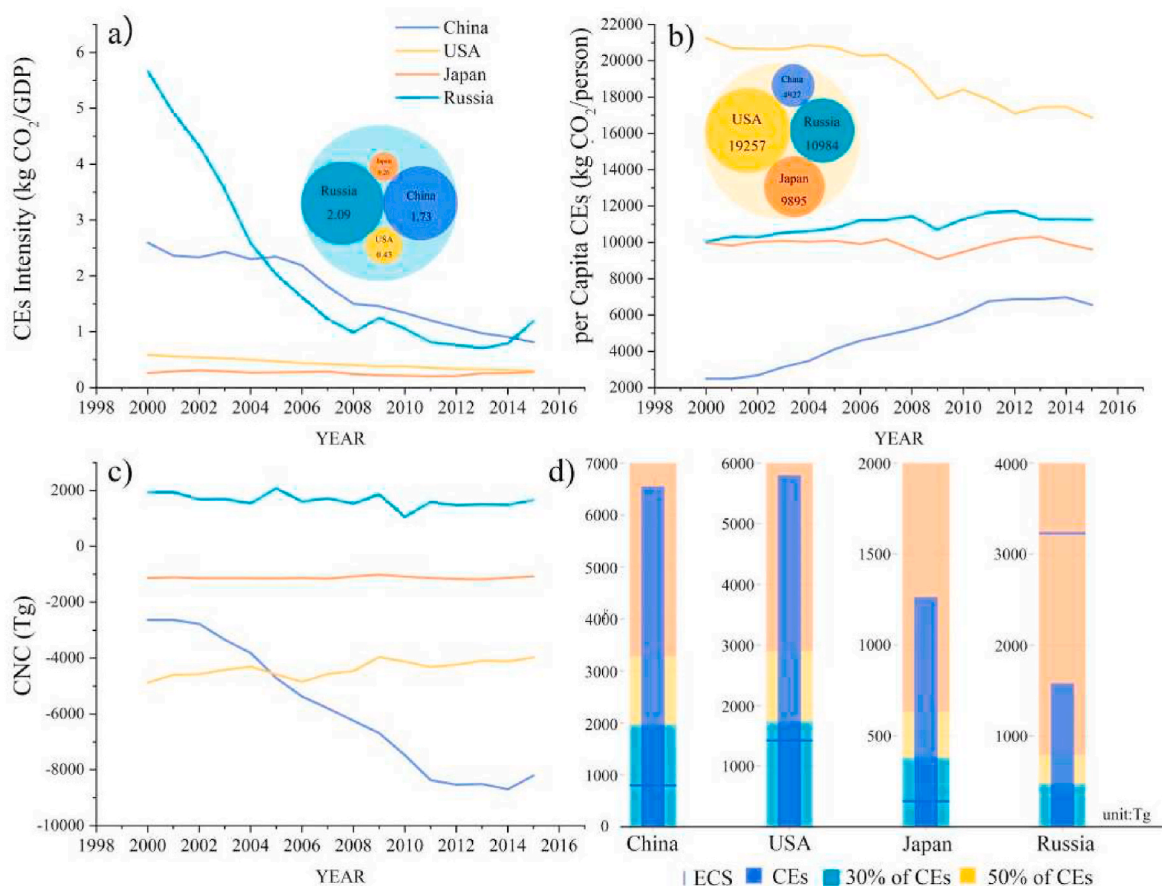
Fig. 6. Carbon emissions (CEs) intensity (a), per capita CEs (b), carbon neutral capacity (CNC) (c), and the relationship (d) between ecosystem carbon sink (ECS) and CEs for China and other countries (the United States, Japan, and Russia).

Fig. 7, the ECS will continue to increase in the future in both scenarios A2 and B1 (Fig. 7b). Under scenario B1, the growth trend of the ECS will be greater than that under scenario A2, which shows that the sustainable development of globalization can not only drive the improvement of the economy and the value of ecological services but also contribute more to the mitigation of global climate change. However, due to global warming and the effect of CO_2 fertilization, the CO_2 absorbed by terrestrial ecosystems under scenario A2 from 2025 to 2060 will be slightly greater than that under scenario B1. In summary, under scenario B1, the terrestrial ecosystem will absorb nearly 21 Tg of CO_2 less than under scenario A2, which is equivalent to the CO_2 emitted by half of Qinghai in 2017.

Since the magnitude of the ECS will be smaller than that of the CEs, the future change in the CN potential will be mainly affected by the changes in the CEs (Fig. 7c). As shown in Fig. 7c, in scenario A2, China's carbon deficit soars from 9.46 Pg in 2025 to 11.33 Pg in 2030. By 2060, China will have 12.5 Pg CO_2 of CEs that need to be eliminated to achieve CN. In scenario B1, China's carbon deficit will be 15.0 Pg, 21.18 Pg, and 7.3 Pg by 2025, 2030, and 2060, respectively. This indicates that although the potential for CN status is going to weaken in the early stage, the sustainable development of globalization may relieve the pressure of reducing emissions to a certain extent during long-term development. From 2017 to 2060, the CN capacities under the two scenarios (A2/B1) will decrease by 44.58% and increase by 15.54%. Among them, under scenario B1, the sharpest decline between 2017 and 2028 may be caused by the failure to find a correct balance between rapid economic development and ecological protection (Liu et al., 2020). In addition, it can be clearly seen that under the two scenarios, the proportion of CEs absorbed by terrestrial ecosystems over time will change along opposite trends (Fig. 7d). This demonstrates that

environmental sustainability can only be achieved through timely technological innovations and the transformation of the production structure and consumption patterns (Liang et al., 2014). The application of clean energy and man-made emissions reduction technologies should be further strengthened. Only with low-carbon industries, buildings, and transportation systems and the implementation of the concept of low-carbon consumption can we achieve future CN goals while taking into account regional poverty alleviation and development. However, in the early stage of promoting sustainable development and clean energy, the cost China needs to pay in terms of CEs is also huge.

4.4. Future perspectives and uncertainty

There is also some uncertainty in the results of this study. First, for the CE measurement, the different statistical standards and units used (Chen et al., 2005, 2009; Pan et al., 2013) caused differences in the CE statistics of the different provinces and countries. In addition, in terms of the prediction of the CN capability, the factors were quite complex and diverse. Although eight representative indicators were selected for the analysis in this study, the impacts of factors such as the energy prices, and environmental regulations on CEs were not considered. This had an impact on the calculation of the CEs. These factors will be incorporated into the model in the future.

Second, when calculating the RCS, due to the difficulty of obtaining the actual runoff on the pixel scale, the calculated runoff depth was deduced from the actual results. Moreover, soil erosion also can influence ECS (Luo et al., 2022). In addition, studies have shown that the error of the soil respiration was between 2% and 4% (Pei et al., 2009). In terms of the simulation and prediction of the carbon sink, the spatial resolution of the CMIP5 and IBIS prediction data was relatively large
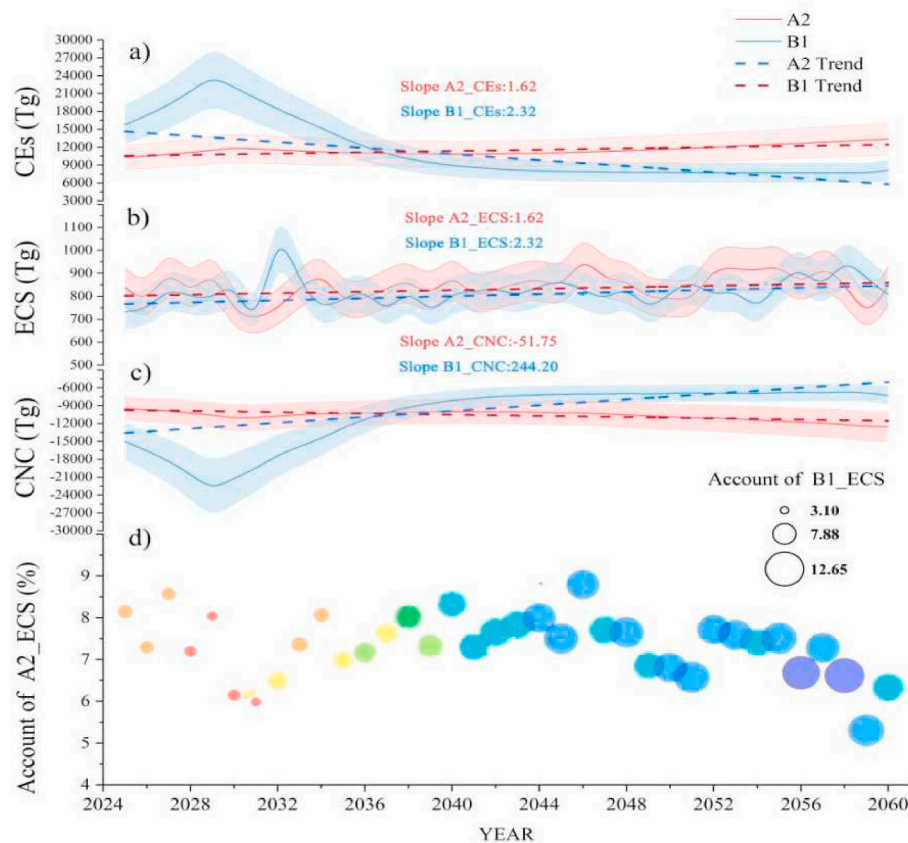
Fig. 7. China's future carbon emissions (CEs) (a), ecosystem carbon sink (ECS) (b), carbon neutral capacity (CNC) (c) under different scenarios (A2 and B1), and (d) ECS as a percentage of CE (the above data exclude Tibet, Hong Kong, Macau and Taiwan).

$(0.5°)$, so the model cannot reflect the details in specific regions in a more detailed manner, including smaller cities such as Shanghai. These issues need to be resolved in future research. Finally, according to the uncertainty model (Landschützer et al., 2014), the uncertainty of the results in this study was between 15.36% and 27.26%. The uncertainty represents the maximum deviation because it is the maximum cumulative uncertainty in all data and models.

5. Conclusion

Based on China's energy emissions data, meteorological and hydrological data in China, lithology data and vegetation data, we used GEM-CO_2 model, soil respiration model, spatial autocorrelation analysis method, neural network model and other methods to reveal the temporal and spatial distribution pattern of ECS in China, explore the differences in CN capacity in different regions of China, and Simulate and predict it under future scenarios. Specific conclusions are as follows:

(1) China's terrestrial ecosystem was a huge carbon sink from 1997 to 2017, and its annual average NEP reached 0.61 Pg CO_2/yr. Furthermore, China's CEs have been rising sharply year by year from 1997 to 2017, with an average annual change rate of 9.81%.
(2) During the study period, annual CEs of 5.63 Pg CO_2 were not absorbed, which is about 90% of CEs.
(3) In China, CNC was generally weakening. Although the CNC of some municipalities were relatively weak, they also maintained a slight upward trend. This showed that the leading edge of China's economic development were trying its best to achieve emission reduction targets.
(4) The cities in China were dominated by high-value and high-value clusters and low-value and low-value clusters. The spatial

boundaries of the distribution of the two were obvious located in the southwest and the Northeast of China respectively. The polarization degree of China's CNC is in a relatively reasonable level.
(5) In the B1 scenario, China's carbon deficit will be 15.0 Pg, 21.18 Pg and 7.3 Pg by 2025, 2030, and 2060, respectively. This proved that although the potential for CN is going to weak in the early stage, the sustainable development of globalization may be relieve the pressure of reducing emissions to a certain extent in the long-term development.

CRediT authorship contribution statement

Sirui Zhang: Conceptualization, Formal analysis, Writing – original draft. **Xiaoyong Bai:** Conceptualization, Supervision, Resources. **Cuiwei Zhao:** Validation, Project administration. **Qiu Tan:** Validation, Project administration. **Guangjie Luo:** Validation, Project administration. **Luhua Wu:** Validation, Formal analysis. **Huipeng Xi:** Validation, Formal analysis. **Chaojun Li:** Validation, Formal analysis. **Fei Chen:** Data curation, Writing – review & editing. **Chen Ran:** Data curation, Writing – review & editing. **Min Liu:** Visualization, Investigation. **Suhua Gong:** Visualization, Investigation. **Fengjiao Song:** Visualization, Investigation.

Declaration of competing interest

The authors declare that they have no known competing financial interests or personal relationships that could have appeared to influence the work reported in this paper.

Acknowledgments

Appendix A. Supplementary data

Supplementary data to this article can be found online at https://doi.org/10.1016/j.jclepro.2022.130966.

References

Ai, X.Q., 2017. Measure wealth inequality: application of Gini Index when negative values exist. Stat. Decis. 4, 3.

Anselin, L., 1995. The local indicators of spatial associatior-LISA. Geogr. Anal. 27, 93115.

Carrie, N.R., Moore, K.R., Keith, S.E.L., 1996. Long-distance homing of a translocated red-cockaded woodpecker. Wildl. Soc. Bull. 24 (4), 607-607.

Chen, Y.J., Sheng, G.Y., Bi, X.H., et al., 2005. Emission factors for carbonaceous particles and polycyclic aromatic hydrocarbons from residential coal combustion in China. Environ. Sci. Technol. 39 (6), 1861–1867.

Chen, Y.J., Zhi, G.R., Feng, Y.L., et al., 2009. Measurements of black and organic carbon emission factors for household coal combustion in China: implication for emission reduction. Environ. Sci. Technol. 43 (24), 9495–9500.

Chen, P.F., et al., 2019. 1-km raster dataset of monthly net primary productivity of terrestrial ecosystems in China north of 18° N (1985-2015). [DB/OL]. Data publishing system for global change science research. https://doi.org/10.3974/geodb.2019.03.02.V1.

Chen, J.D., Cheng, S.L., Song, M.L., et al., 2016. Interregional differences of coal carbon dioxide emissions in China. Energy Pol. 96, 1–13.

Chen, J., Gao, M., Cheng, S., et al., 2020. County-level CO_2 emissions and sequestration in China during 1997–2017. Sci. Data 7, 391. https://doi.org/10.1038/s41597-020-00736-3.

Ciais, P., Sabine, C., Bala, G., et al., 2013. Carbon and Other Biogeochemical Cycles. Cambridge University Press, London.

Clarke-Sather, A., Qu, J.S., Wang, Q., et al., 2011. Carbon inequality at the sub-national scale: a case study of provincial-level inequality in CO_2 emissions in China 1997-2007. Energy Pol. 39, 5420–5428.

Cumming, G.S., von Cramon-Taubadel, S., 2018. Linking economic growth pathways and environmental sustainability by understanding development as alternate social-ecological regimes. Proc. Natl. Acad. Sci. U.S.A. 115, 9533–9538.

Development Research Center of the State Council (DRCSC), 2005. Investigation Report: Strategic thinking and policy measures to achieve coordinated development among regions. https://www.drc.gov.cn/DocView.aspx?chnid=386&leafid=1339&docid=30955.

Diakoulaki, D., Mavrotas, G., Orkopoulos, D., et al., 2006. A bottom-up decomposition analysis of energy-related CO_2 emissions in Greece. Energy 31, 2638–2651.

Fang, J.Y., 2000. Forest biomass carbon pool of middle and high lati-tudes in the North Hemisphere is probably much smaller than presentestimates (in Chinese). Acta Phytoecol. Sin. 24 (5), 635–638.

Fang, J.Y., Guo, Z.D., Piao, S.L., 2007. Estimation of China's terrestrial vegetation carbon sink from 1981 to 2000 (in Chinese). Sci. China E 37 (6), 804–812.

Foley, J.A., 1995. An Equilibrium model of the terrestrial carbon budget. Tellus 47, 3102319.

Friedlingstein, P., Jones, M.W., O'Sullivan, M., et al., 2019. Global carbon budget 2019. Earth Syst. Sci. Data 11, 1783–1838.

Gong, S.H., Wang, S.J., Bai, X.Y., et al., 2020. Response of the weathering carbon sink in terrestrial rocks to climate variables and ecological restoration in China. Sci. Total Environ. 750, 141525.

Goulden, M.L., Wofsy, S.C., Harden, J.W., et al., 1998. Sensitivity of boreal forest carbon balance to soil thaw. Sci. 279 (5348), 214–217.

Hartmann, J., Moosdorf, N., 2012. The new global lithological map database GLiM: a representation of rorties at the Earth surface. G-cubed. https://doi.org/10.1029/2012GC004370.

Hatfield-Dodds, S., Schandl, H.P., Adams, D., et al., 2015. Australia is 'free to choose' economic growth and falling environmental pressures. Nature 527, 49–53.

He, X.B., 2019. Study on the Prediction of Carbon Emission Peak in China (In Chinese). North China Electric Power University, Beijing.

Intergovernmental Panel on Climate Change (IPCC), 2000. IPCC special report emission scenarios: summary for policymakers. https://ar5-syr.ipcc.ch/topic_summary.php.

Intergovernmental Panel on Climate Change (IPCC), 2006. 2006 IPCC Guidelines for National Greenhouse Gas Inventories.

Kendall, M.G., 1975. Rank Correlation Methods, fourth ed. Charles Griffin, London, p. 272.

Landschützer, P., Gruber, N., Bakker, D.C.E., Schuster, U., 2014. Recent variability of the global ocean carbon sink. Global Biogeochem. Cycles 28, 927–949.

Lapenis, A., Klene, A., 1997. Conveyor of live germs. Eos Trans. AGU 78 (34), 359-359.

Li, Z.K., 2021. Empirical analysis on the change of industrial structure to economic growth in the 30th anniversary of the establishment of Hainan Province. China Circ. Econ. 1, 100–103.

Li, H.W., Wang, S.J., Bai, X.Y., et al., 2018. Spatiotemporal distribution and national measurement of the global carbonate carbon sink. Sci. Total Environ. 643, 157–170.

Liang, S., Liu, Z., Crawford-Brown, D., et al., 2014. Decoupling analysis and socioeconomic drivers of environmental pressure in China. Environ. Sci. Technol. 48, 1103–1113.

Lin, B.Q., Benjamin, N.I., 2017. Influencing factors on carbon emissions in China transport industry. A new evidence from quantile regression analysis. J. Clean. Prod. 150, 175–187.

Liu, Z.H., 2000. Contribution of carbonate rock weathering to atmospheric CO_2 sink (in Chinese). Carsol. Sin./Zhong Guo Yan Rong 19 (4), 293–300.

Liu, Z.H., Zhao, J., 2000. Contribution of carbonate rock weathering to the atmospheric CO_2 sink. Environ. Geol. 39 (9), 1053–1058.

Liu, H., Nie, J., Cai, B., 2019. CO_2 emissions patterns of 26 cities in the Yangtze River Delta in 2015: Evidence and implications. Environ. Pollut. 252, 1678–1686.

Liu, S.W., Tian, X., Xiong, Y.L., et al., 2020. Challenges towards carbon dioxide emissions peak under in-depth socioeconomic transition in China: insights from Shangha. J. Clean. Prod. 247, 119083.

Luo, X.L., Bai, X.Y., Tan, Q., Ran, C., Chen, H., Xi, H.P., Chen, F., Wu, L.H., Li, C.J., Zhang, S.R., Zhong, X., Tian, S., 2022. Particulate organic carbon exports from the terrestrial biosphere controlled by erosion. Catena 209 (1), 105815.

Lv, Y., Dong, G.T., Yang, S.T., et al., 2014. Spatio-temporal variation in NDVl in the Yarlung Zangbo river basin and its relationship with precipitation and elevation (in Chinese). Resour. Sci. 36 (3), 603–611.

Lythgoe, K.A., Morrison, L.J., Read, A.F., et al., 2007. Parasite-intrinsic factors can explain ordered progression of trypanosome antigenic variation. Proc. Natl. Acad. Sci. U.S.A. 104, 8095–8100. https://doi.org/10.1073/pnas.0606206104.

Mallapaty, S., 2020. How China could be carbon neutral by mid-century. Nature 586, 482–483.

Mann, H.B., 1945. Non-parametric tests against trend. Economy 13, 245–259.

Martin, J.B., 2017. Carbonate minerals in the global carbon cycle. Chem. Geol. 449, 58–72.

Moran, P.A.P., 1950. Notes on continuous stochastic phenomena. Biometrika 37 (1–2), 17–23.

National Bureau of Statistics of China (NBSC), 2021. China statistical year book. https://data.stats.gov.cn/english/publish.htm?sort=1.

Pacala, S.W., Hurtt, G.C., Baker, D., et al., 2001. Consistent land- and atmosphere-based US carbon sink estimates. Sci. 292, 2316–2320.

Pan, Y., Birdsey, R.A., Fang, J., et al., 2011. A large and persistent carbon sink in the world's forests. Sci. 333, 988–993.

Pan, K.X., Zhu, H.X., Chang, Z., et al., 2013. Estimation of coal-related CO_2 emissions: the case of China. Energy Environ. 24 (7–8), 1309–1321.

Pei, Z., Ouyang, H., Zhou, C., et al., 2009. Carbon balance in an alpine grassland ecosystemon the Tibetan Plateau. J. Integr. Plant Biol. 51 (5), 521–526.

Peng, S.Z., Ding, Y.X., Liu, W.Z., et al., 2019. 1 km monthly temperature and precipitation dataset for China from 1901 to 2017. Earth Syst. Sci. Data 11, 1931–1946. https://doi.org/10.5194/essd-11-1931-2019.

Piao, S.L., Fang, J.Y., Ciais, P., et al., 2009. The carbon balance of terrestrial ecosystems in China. Nature 458, 1009–1013.

Ping, X.Q., Zheng, Y.M., Cao, H.P., 2020. The change trend of carbon emission intensity in China and the policy optimization of carbon emission reduction during the 14th five-year plan period (in Chinese). Reform 11, 37–52.

Pu, J.B., Jiang, Z.C., Yuan, D.X., et al., 2015. Some opinions on rock-weathering-related carbon sinks from the IPCC fifth assessment report (in Chinese). Adv. Earth Sci. 30 (10), 1081–1090.

Qiu, D.S., Zhuang, D.F., Hu, Y.F., et al., 2004. Estimation of carbon sink capacity caused by rock weathering in China (in Chinese). Earth Sci. 29 (2), 177–182.

Qu, S.N., Guo, C.X., 2010. Forecast of China's carbon emissions based on STIRPAT model. China Popul. Resour. Environ. 20 (12), 10–15.

Rumelhart, D.E., Mcclelland, J.L., 1987. Feature Discovery by Competitive Learning. MIT Press, Massachusetts.

Running, S., Mu, Q., Zhao, M., 2015. MOD17A3H MODIS/Terra gross primary productivity yearly L4 global 500m SIN grid. NASA LP DAAC. http://doi.org/10.5067/MODIS/MOD17A3H.006.

Solomon, S.D., Qin, M., Manning, Z., et al., 2007. Couplings Between Changes in the Climate System and Biogeochemistry. In: Climate Change 2007: The Physical Science Basis. London: Cambridge University Press, London, pp. 499–587.

Song, J.K., Zhang, Y., 2011. Scene prediction of China's carbon emissions based on BP neural network (in Chinese). Sci. Technol. Eng. 11 (17), 254–257.

Suchet, P.A., Probst, J.L., Ludwig, W., 2003. Worldwide distribution of continental rock lithology: implications for the atmospheric/soil CO_2 uptake by continental weathering and alkalinity river transport to the oceans. Global Biogeochem. Cycles 17, 1038.

Talukdar, D., Meisner, C.M., 2001. Does the private sector help or hurt the environment? Evidence from carbon dioxide pollution in developing countries. World Dev. 29, 827–840.

Tao, Z., Gao, Q.Z., Liu, K., 2011. Carbon sequestration capacity of the chemical weathering processes within drainage basins (in Chinese). Quat. Sci. 31 (3), 408—416.

Walter, H., 1994. Vegetation of the Earth, third ed. Springer, New York.

Wang, A.L., Lin, B.Q., 2017. Assessing CO_2 emissions in China's commercial sector: determinants and reduction strategies. J. Clean. Prod. 164, 1542–1552.

Wang, S.J., Fang, L.C., Sun, L.X., et al., 2018. Decarbonizing China ' s urban agglomerations. Ann. Assoc. Am. Geogr. 109 (1), 1–20.

Woodwell, G.M., Whittaker, R.H., Reiners, W.A., 1978. The biota and the worldcarbon budget. Science 199, 141–146.

Worthington, E., 1965. The international biological programme. Nature 208, 223–226.

Xi, X.P., Xie, Y.S., Wang, H.L., et al., 2014. Forecast of Jiangxi's carbon emissions to peak based on IPAT model (in Chinese). Jiangxi Sci. 32 (6), 768–772.

Xi, H.P., Wang, S.J., Bai, X.Y., et al., 2021. The responses of weathering carbon sink to eco-hydrological processes in global rocks. Sci. Total Environ. 788, 48–9697.

Xu, S.Y., Jiang, Z.C., 1997. Preliminary estimation of the relationship between karstification in my country and the sources and sinks of atmospheric greenhouse gas CO_2 (in Chinese). Chin. Sci. Bull. 42 (9), 953–955.

Yang, S.S., 2017. Regional carbon emissions estimation and scenario analysis in the Yangtze river economic belt (in Chinese). Ecol. Econ. 33 (9), 26–30.

Yang, J., Hao, Y., Feng, C., 2021. Increased inequalities of per capita CO_2 emissions in China. Sci. Rep. 11, 9358.

Zhang, M., Huang, X.J., Chuai, X.W., 2020. Spatial distribution and changing trends of net ecosystem productivity in China. Geogr. Geo-inf. Sci. 36 (2), 69–74.

Zhen, Z., Hong, J., Liu, J., et al., 2013. Effect of heterogeneous atmospheric CO_2 on simulated global carbon budget. Global Planet. Change 101, 33–51.

Zheng, L.X., 2005. The old road of traditional heavy chemical industry cannot be taken. Econ. Dail. 9.

Zhou, W., Mi, H., 2010. Calculation on energy-related coemissions in China (2010~2050) (in Chinese). China Environ. Sci. 30 (8), 1142–1148.